Handbook on the Emerging Trends in Scientific Research
ISBN: 978-969-9952-05-0
homepage: http://www.pakinsight.com/?ic=book_detail&id=10
Conference venue : Pearl International Hotel, Kuala Lumpur, Malaysia
Vol.3 , 2015
(25-26, April)

# Synthesis of Clay-Based Ceramic/Carbon Composite by Starch Consolidation Casting and Reductive Sintering

**Alexander O. Mosqueda[1] --- Ruben L. Menchavez[2] --- Nathaniel M. Anacleto[3]**

[1]*Department of Chemical Engineering and Technology, Mindanao State University-Iligan Institute of Technology, Iligan City, Philippines*
[2,3]*Department of Ceramic, Metallurgical and Mining Engineering, Mindanao State University-Iligan Institute of Technology, Iligan City, Philippines*

## Abstract

This study explores a method of synthesizing a clay-based ceramic/carbon composite by starch consolidation casting followed by low-temperature reductive sintering. The ceramic slurry was prepared from a ternary powder mixture of 46.7 wt% Lama-lama clay, 18.00 wt% quartz and 35.30 wt% feldspar. The slurry was consolidated with 16.0 wt% potato starch in a mould heated inside a pressure cooker to obtain cylindrical green bodies. The well-dried samples were then sintered at temperatures from 1000$^{o}$C to 1250$^{o}$C in a vertical tube furnace under a constant flow of argon gas. The sintered samples contained a varying amount of pyrolyzed carbon (3.96-1.27%) that formed conduction networks. Correspondingly, the physical properties were evaluated for the sintered samples. The measured electrical conductivity of the sintered samples was found to increase from 0.85 to 3.91 S/cm with increasing sintering temperature. The X-ray Diffraction analysis of the sintered samples disclosed that the pyrolyzed carbon was a graphite phase associated with mullite, wustite and other ceramic phases. These findings were supported with Scanning Electron Microscopy (SEM) with Energy Dispersive X-ray Spectroscopy (EDS). Hence, the clay-based ceramic/carbon composite is a potential candidate for use as a carbon-filled ceramic water filter or as electrode materials.

**Keywords:** Ceramic/carbon composite, Clay-based, Carbon yield, Reductive sintering.

## 1. Introduction

Ceramic/carbon composites are used in a variety of industrial applications such as components for space vehicles, gas turbines, burners, brake discs, slide bearings and reactors. These ceramic composites are commonly considered to be alternative materials over the conventional technical ceramics owing to their enhanced physical and chemical properties. Most of the approaches for fabricating these ceramic composites are successfully demonstrated with a reaction-bonded technique that involves infiltration of a carbon preform with molten/gaseous ceramic (e.g. silicon) at high temperature in an inert atmosphere (Vyshnyakova *et. al*., 2006). Another unique shaping method is utilizing a gelcasting method followed by inert sintering of gel-bound ceramics to yield a pyrolyzed carbon in ceramic matrix. This method utilizes slurry of ceramic powder in a solution of organic monomer that polymerizes to form a strong, cross-linked solvent polymer gel filled with the ceramic powder (Menchavez et. al., 2008). However, this method suffers undesirable disadvantage of high toxicity to human health due to the use of synthetic monomers and other chemical reagents.

To address the aforementioned processing issues, the starch is commonly used as a consolidating agent of slurry loaded with a high amount of ceramic powder. The starch is a natural biopolymer made up of amylose and amylopectin units. When the starch particles are mixed in ceramic slurry, the consolidation happens due to its swelling and gelling properties. This phenomenon preferably takes place during heating at a temperature of 60-80$^{o}$C, leading to swelling of the starch granules due to water uptake. The water content of the slurry slowly decreases, causing the ceramic particles to stick together and eventually consolidate into a green body (Lyckfeldt and Ferreira, 1998). The consolidated body is finally heated to remove the gelatinized starch, which is subsequently sintered at high temperature to increase the mechanical strength. Since the starch particles occupy spaces in the ceramic compact, it serves as a pore former that can easily be burned out during heat treatment in air to fabricate porous ceramics. This forming technique has commonly been employed to consolidate pure and impure inorganic powders.

The complete removal of starch particles from the ceramic compact by oxidation heating results in an undesirable volume of gaseous emissions. To mitigate this problem, a reductive heating is employed to offer a new attractive route to synthesize homogeneous carbon-based materials. Particularly, it has been reported elsewhere that the starch is used as a precursor for the preparation of carbon spheres and

activated carbon. These carbon-based materials are obtained through the pyrolysis of starch particles impregnated with a chemical agent to increase the carbon yield. The carbonized starch particles have a spherical morphology with well-developed pore structures (Zhao *et. al.*, 2008). This carbonization technology of starch presents a new avenue in shaping a homogeneous ceramic/carbon composite while the starch is used as the consolidating agent.

The starch consolidation technique has been firstly reported to produce carbon/ceramic composite using pure alumina compact that is thermally treated under reducing atmosphere (Menchavez et al, 2014). Although this method is successful in shaping highly electrically conductive porous ceramics, the use of pure powder presents high energy cost due to a very high sintering temperature and expensive ceramic powder. To the best of the author's knowledge, the starch consolidation technique has not yet been employed to fabricate carbon-based ceramic composites using impure inorganic powders such as mining wastes and locally available ceramic raw materials. Particularly, a red clay-based powder mixture is reported elsewhere to produce porous ceramics compacted by the gelatinization of starch with subsequent binder burnout in air atmosphere. The ceramic mixture primarily consists of dominant amount of red clay, and additive amounts of quartz and feldspar. The clay, naturally containing iron impurity, imparts plasticity and reddish color to the powder mix while the quartz provides filler and feldspar allows low firing temperature to reduce energy requirement (Menchavez and Itong, 2008). Hence, this clay-based mixture offers the use of cheaper raw materials and low energy for thermal treatment as compared to pure inorganic powders.

The present study, therefore, explores a method of preparing a clay-based ceramic/carbon composite by starch consolidation casting followed by a low-temperature reductive sintering. The gelatinized starch particles that consolidate the ceramic particles are harnessed as precursor for the carbon material by in-situ pyrolysis under argon atmosphere. This process results in a sintered ceramic composite made of red clay-based ceramic and pyrolyzed carbon. The presence of such carbon was determined by measuring the electrical conductivity and carbon yield. Correspondingly, the phases of the pyrolyzed carbon and the associated ceramic phases were determined by X-ray diffraction analysis supported with Scanning Electron Microscopy (SEM) with Energy Dispersive X-ray Spectroscopy (EDS). The pyrolyzed carbon is expected to be uniformly distributed within the ceramic body, which has direct implications on the chemical and physical properties of the sintered ceramic composite. This process presents a simple, less expensive and eco-friendly approach to prepare a carbon-filled ceramic composite.

# 2. Experimental

## 2.1. Starting Materials

A dried red clay (from Lama-Lama, Lanao del Norte, Philippines) was crushed in a pulverizer to reduce its lumped size. Further milling in a ballmill was done to achieve the desired particles sizes with subsequent sieving through a 100 mesh screen. Silica quartz, feldspar and potato starch were locally available from a chemical supplier with average particle sizes (LS 100Q, Coulter Corporation) of 35.1, 27.0, and 40.9 μm, respectively. A Sodium tripolyphosphate (STTP) was used as the dispersing agent.

## 2.2. Sample Preparation

A powder mixture was prepared composed of 46.70 wt% red clay, 35.30 wt% feldspar, and 18.00 wt% quartz. The mixture was dispersed in distilled water (70% solid loading) by ball milling for 4 h with 0.7 wt% sodium tripolyphosphate (STTP) as the dispersing agent. After 4 h, the dispersed ceramic slurry was loaded with 16 wt% potato starch based on the mass of powder mixture and further milled for 4 h to homogenize the ceramic-starch slurry. The starch-loaded ceramic slurry was cast into a cylindrical mold made of acetate in a beaker and heated in a pressure cooker for 12-15 minutes. The heating happened through the produced steam under high pressure. The pressure cooker has a maximum pressure of 15 psi (103kPa) above the atmospheric pressure that allows the steam temperature to reach up to 121$^{o}$C (250$^{o}$F) during heating as stated in the user manual. The solidified green bodies were demoulded and dried at room temperature for a week, and then oven dried at 110$^{o}$C. The dried and polished green bodies were sintered at 1000, 1150, 1200 and 1250$^{o}$C for 1 h under 0.5L/min of argon with a heating rate of 10$^{o}$C/min.

## 2.3. Reductive Sintering

A vertical tube furnace (LABEC Pty Ltd) was employed for the reductive heat treatment of the samples under inert condition. After the drying step, the samples were polished to a symmetric cylindrical shape using a sand paper. The polished samples were placed in a sample container made of alumina crucible and loaded into the tube furnace. Before heating, the furnace was purged with Ar gas for 30 minutes to free the tube from oxygen that might interfere in the reduction process. Then, the samples were heated at 1200$^{o}$C with a heating rate of 10$^{o}$C/min under 0.5 L/min of Ar (Ultrahigh Purity, UHP 99.999%). The sintering temperature was chosen based on the previous studies on processing of lama-lama clay, in which, the effective firing temperature was at 1050$^{o}$C-1250$^{o}$C (Menchavez, et. al., 2013).

## 2.4. Physical Characterizations

The linear shrinkage of the sintered samples was calculated by equation 1 with the heights (in mm) of the cylindrical sample before ($H_o$) and after ($H_f$) reductive sintering.

$$\% LS = \frac{(H_o - H_f)}{H_o} x\ 100\% \qquad (1)$$

The bulk density and apparent porosity of the sintered bodies were measured by Archimedes method.

The biaxial tensile strength was determined using a versa-loader machine (Model G-900-4, ELE International SOILTEST Products Division). The breaking force, y was obtained by the equation below:

$y = 4.466171x - 25.061$ (2)

where x is the dial reading on the machine multiplied by 10 divisions. The biaxial tensile strength, σ (in psi) was calculated using equation 3 where y is breaking force, D is the sample diameter and T is the sample thickness.

$$\sigma = \frac{2y}{\pi DT} \quad (3)$$

The carbon yield was determined by thermogravimetric analysis (STA 6000 Perkin Elmer) at 30-900$^{o}$C with a heating rate of 10$^{o}$C/min under oxygen atmosphere. The phase composition and microstructure of the sintered samples were examined by XRD, and SEM (JSM-6100, JEOL).

Electrical conductivity measurements were conducted on plate samples and evaluated using a Van der Pauw method. The bulk samples sintered at different temperatures were cross-sectioned using a Digital Precision Diamond Saw (Topper CL-50) to obtain the desired dimension of the plate (14.5 mm x 14.5 mm x 2.5 mm). The bulk resistivity (ρ) of the plates was calculated using equation 4.

$$\rho = \left(\frac{\pi d}{ln\ 2}\right)\left[\frac{R_A + R_B}{2}\right] f(R_A, R_B) \quad , \Omega cm$$

$$f(R_A, R_B) \cong 1 - \left[\frac{R_A - R_B}{R_A + R_B}\right]^2 \left(\frac{ln\ 2}{2}\right) - \left[\frac{R_A - R_B}{R_A + R_B}\right]^4 \left[\frac{(ln2)^2/4 - (ln2)^3}{12}\right]$$

$R_A > R_B$ (4)

where *d* is the thickness of the plate, $R_A$ and $R_B$ are the surface resistances, and *f* ($R_A$ and $R_B$) is the geometric factor. The electrical conductivity (S/cm) of the sintered sample is the inverse of the bulk resistivity.

## 3. Results and Discussion

The cylindrical green bodies were successfully formed from the consolidation of clay-based ceramic mixture with the starch. The ceramic body has a light brown color after the processing steps involving pressure cooking, air, and oven drying, as shown in figure 1a. It can be observed that the reductive heating of the well-dried samples at any sintering temperatures results in the transformation of the color to black (figure 1b). This observation strongly indicates the presence of a significant amount of pyrolyzed carbon retained in the ceramic matrix. In the reductive heating of starch particle in the ceramic matrix, sequential thermal events take place, involving dehydration, rearrangement, and evolution of $CO/CO_2$. The thermal events lead to the formation of carbonaceous residue as reflected in the carbon content when the heating temperature approaches 1000$^{o}$C.

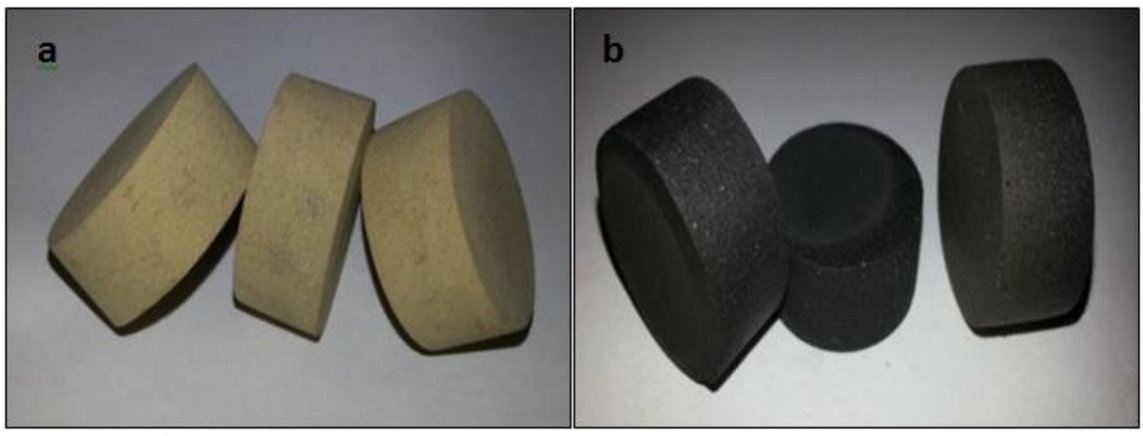


**Figure-1.** Physical appearance of the a) dried ceramic bodies and b) sintered ceramic bodies.

The presence of carbon in the ceramic matrix is expected to influence the physical properties of the sintered composites. Figure 2 shows the relative linear shrinkage of the fired samples against varying sintering temperature. It can be observed that the linear shrinkage is increasing as the sintering temperature is increased. This is attributed to the effect of high temperature on the volume of the material that decreases due to the combined effect of thermal compaction of ceramic particles and movement of the melted particles into the pores and interstices between ceramic particles. This mechanism leads to densification and reduced porosity of the ceramic body (Al-Lami, 2008). The pores are generally attributed to the empty spaces left by the starch particles during reductive burnout. This burnout is represented by the other elements that compose the starch, such as hydrogen and oxygen. During this reductive burnout, the carbon is deposited on the surfaces of the ceramic particles to form conduction networks. Furthermore, the atomic diffusion from low melting phases in the ceramic mixture is a more effective mechanism to join ceramic particles at high temperatures as the material transport is dominating to fill pore spaces and interstices. This results in the significant increase of the linear shrinkage from 3.42% to 6.51%. The resulting trend of linear shrinkage against the measured apparent porosity is inversely related to each other at increasing sintering temperature. The obtained trend for the measured apparent porosity decreases from 46.46% to 27.98% as sintering temperature increases, as depicted in figure 3.

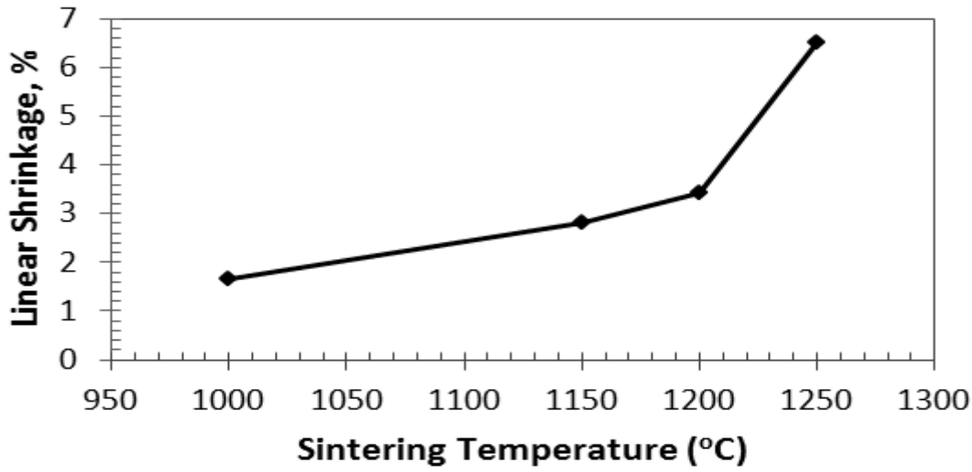


**Figure-2.** Linear shrinkage of the fired samples against varying sintering temperature.

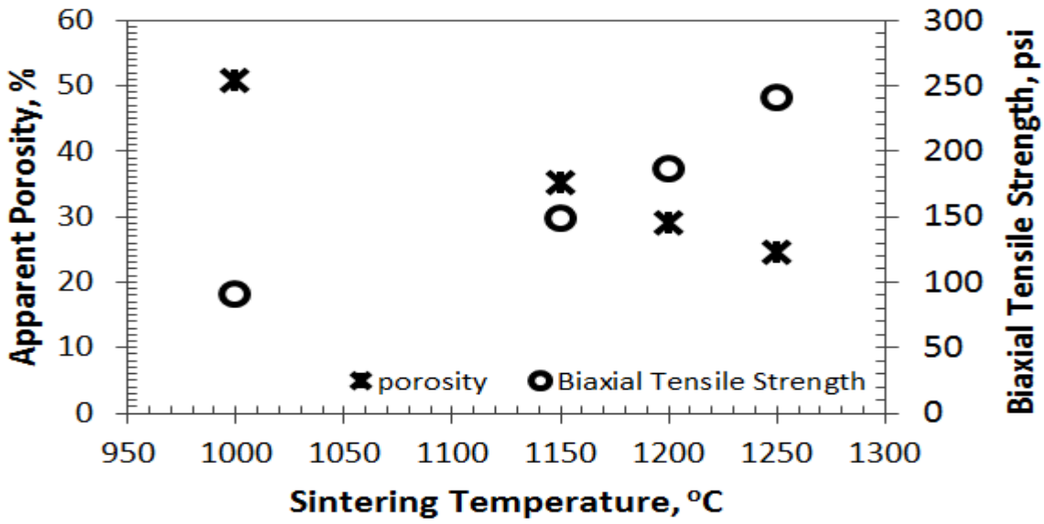


**Figure-3.** Apparent porosity and biaxial tensile strength of the fired samples against varying sintering temperature.

The increase in linear shrinkage and the reduction of apparent porosity have a direct implication on the mechanical property of the sintered body. As shown in figure 3, the biaxial tensile strength increases from 90.52 psi to 240.03 psi with increasing sintering temperature. The increase in mechanical strength is related to the decrease in the porosity of the fired sample while the solid part increases for mechanical support. The lowering of porosity means that more pores were eliminated and the ceramic body becomes more densified and compact, resulting to a higher mechanical strength. This densification was also supported by the data obtained for the bulk density in figure 4, which increases with sintering temperature.

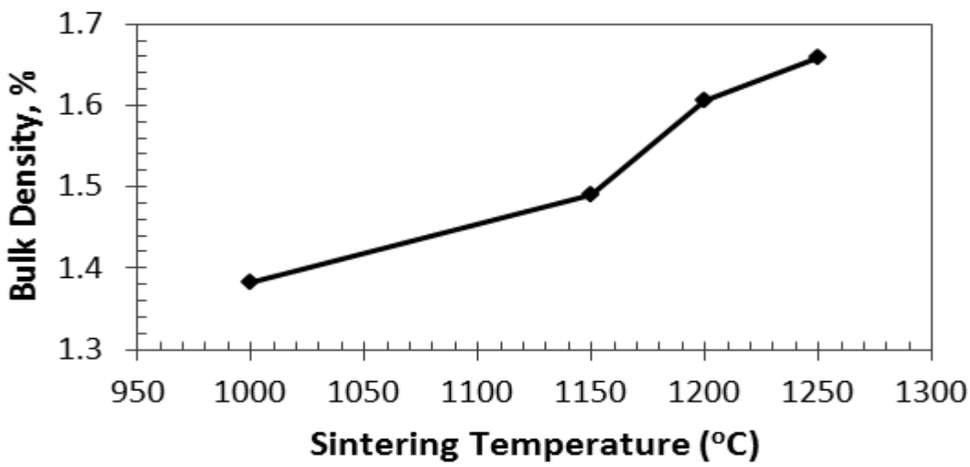


**Figure-4.** Bulk density of the fired samples against varying sintering temperature.

The measured physical properties above are strongly affected by the presence of a considerable amount of pyrolyzed carbon in the ceramic matrix. Table 1 tabulates the amount of carbon as a function of the sintering temperature for the sintered samples. A maximum of the carbon yield at about 3.96% was obtained. It can be deduced that during the reductive heating at that temperature there was no significant reaction between the carbon and the ceramic matrix. It is worthwhile to point out that the weight loss due to the oxidized carbon was taken as the amount of carbon retained in the ceramic composite during oxidation heating. However, as the sintering temperature was further increased above 1000$^{o}$C, the carbon yield noticeably decreases to 1.27%. This is because of the fact that the sintering above the temperature of

1000°C causes a thermal scission of glycosidic bonds between the glucose pyranose units of the starch. This mechanism produces many oxygenated compounds to readily react with the pyrolyzed carbon. This reaction produces more $CO/CO_2$, which significantly reduces the amount of carbon retained in the ceramic matrix (Zhao *et. al*., 2008). Also, it is possible that low melting ceramic particles react with carbon to form carbides and carbon-based gases at high temperature. However, the detection of these carbides by X-ray diffraction is hampered due to their small concentration in the ceramic matrix.

**Table-1.** Carbon content of the samples sintered at 1000-1250°C.

| Sintering Temp. | Carbon Yield, % |
|---|---|
| 1000°C | 3.957 |
| 1150°C | 3.385 |
| 1200°C | 2.833 |
| 1250°C | 1.273 |

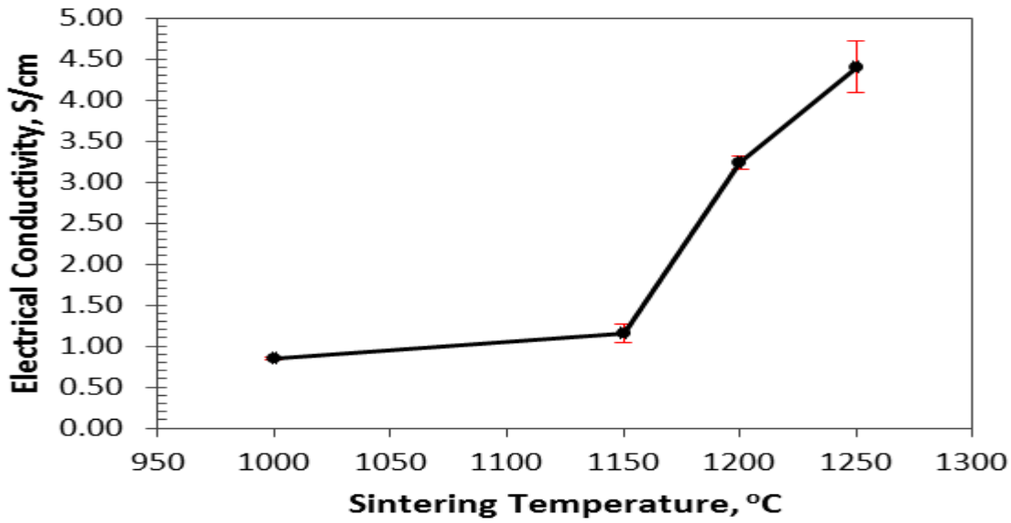


**Figure-5.** Measured electrical conductivity of the samples sintered at 1000-1250 °C.

The presence of the pyrolyzed carbon in the ceramic matrix is thought to form conduction networks in the naturally insulating ceramics. Figure 5 shows the measured electrical conductivity (0.85-3.91 S/cm) of the sintered samples at varying sintering temperature. The high values of the electrical conductivity of the sintered samples confirm that the conduction paths are intact in the originally insulating ceramic matrix. It can be observed that the measured electrical conductivity is significantly increasing as the temperature is increased. This finding is contrary to the trend that the electrical conductivity decreases as the carbon content decreases with increasing sintering temperature. The decrease in carbon content means a few conductive networks are involved in the conduction process. Surprisingly, in this study, the electrical conductivity of the sintered samples increases despite the reduction in the carbon content. It is believed that there might be other conductive phases that reinforced the conduction networks. Also, the observed increase in electrical conductivity of sample sintered at 1150°C could be attributed to the combined effect of the phase of carbon networks and thermal compaction of the particles. As the sintering temperature increases, the graphitization becomes more effective and so the electrical property of the composite is improved (Fuji et. al., 2009). The high degree of graphitization of carbon materials is likely catalyzed by the ceramic host while the sintering temperature is increased, which results in the enhancement of the electrical conductivity.

It was determined that the electrical conductivity of sintered samples is dependent upon the phases formed during reductive treatment. The XRD patterns of the sintered composites heat-treated under the reducing atmosphere at 1000°C and 1150°C are shown in figure 6. It can be observed in the diffractogram the intensified peaks representing a graphite phase in the composites sintered at both temperatures. Interestingly, the graphite phase of the pyrolyzed carbon was formed at the low sintering temperature. The graphitization of common carbon materials usually takes place at 2000°C and even at 3000°C, when using a polymer precursor. It is postulated in this study that the clay particles rendered a catalytic effect in the formation of graphite from the pyrolyzed starch. As discussed above, there are other factors that influence the increase in the electrical property of the sintered composites. The reduction in the carbon content with the increasing sintering temperature normally decreases the electrical conductivity of the sintered samples. Surprisingly, in this study, the electrical conductivity of the sintered samples continues to increase with increasing sintering temperature. The analysis of the diffractograms in figure 6 revealed discernable peaks that can be assigned to wustite (FeO) with more intense peaks in composite sintered at 1150°C. The presence of this phase confirmed the strong reinforcement of this phase to the depleting carbon networks due to the reduction of carbon content. The wustite may have contributed the electrical conductive behaviour of the sintered composite samples. It was reported that FeO have a conductive effect on a slag of $CaO\text{-}MgO\text{-}SiO_2\text{-}Al_2O_3$ that increases with the increase of temperature (Sun and Guo, 2011). Also, the increase in electrical conductivity of the sintered composite can also be attributed to the decreasing porosity of the sintered sample. The pores in the bulk sample will somehow disrupt the continuity of the carbon networks. When the sample is less porous, there is more continuity in the conduction path enhancing the possible flow of electricity (Adachi *et. al*., 2007).

Further analysis of the diffractogram in figure 7 revealed other ceramic phases with labeled peaks assigned to the minerals of quartz and albite of feldspar. These phases present in the composite sintered at both temperatures. Moreover, the presence of mullite phase was detected at both temperatures. This phase becomes more crystalline at 1200-1600$^{o}$C, which gives sharper peaks in its diffraction pattern (Treadwell *et. al*, 1996). In this study, the mullite phase begins to appear at 1000$^{o}$C and becomes more evident at 1150$^{o}$C. XRD analysis was not conducted for samples sintered at 1200$^{o}$C and 1250$^{o}$C due to time and financial constraints. The occurrence of mullite at low temperature is may be attributed to the catalytic effect of the aluminosilicate particles in the clay-based mixture. The catalytic mechanism of the ceramic particles facilitated the rearrangement of amylose and amylopectin structure of the starch to form graphene structures. Also, the ceramic particles may have facilitated the removal of hydroxyl groups and oxygen from the glucose units of starch to favor the graphitization at low temperature. The clay particles, specifically kaolin, are widely used as catalysts for various processes such as catalytic cracking, hydrocracking, alkylation, isomerization, hydrogenation, reforming, ring opening, dimerization esterification, polymerization, etc. (Choudhury *et. al*., 2011).

The sintered composites in this study exhibited considerably higher bulk porosity above 30%. This porosity is attributed to empty spaces left by starch particles during reductive burnout as shown in figure 7. The pores seem to be in irregular shapes, which is typical of a ceramic body formed by the starch consolidation of impure inorganic powder. The progression of the porous microstructures sintered from 1000$^{o}$C to 1250$^{o}$C is depicted in figures 7a to d. It can be observed that large pores are visible, which are surrounded with cell struts at 1000$^{o}$C. As the sintering temperature increases, the cell strut increases in thickness while the pores are shrinking in size. The increasing cell strut provides the increasing mechanical strength of the ceramic composite due to an enhancement of the mechanical support.

Furthermore, in figure 7b, a selected point was chosen for EDS analysis for the ceramic composite sintered at 1150$^{o}$C. Using the EDS result, a low aluminum/silica ratio is obtained corresponding to the mullite phase. The formed mullite is seen to have the morphology of small scale crystals. This observed feature is most likely the same morphology of the mullite phase described in previous studies involving porcelain stoneware bodies (Marquez *et. al.*, 2010). Also, there is another type of mullite consists of needle-like crystal which is formed at 1200-1400$^{o}$C. However, it was not observed in the obtained SEM images. Moreover, a quartz phase is clearly distinct on the point selected as indicated by a high silica ratio. In figure 7c, the iron to oxygen ratio on the point selected signaled the presence of wustite phase with a very intense peak for iron in its EDS spectra. In the same figure, shows the graphene sheets of graphite that is a platelet-like crystalline form of carbon adhering to mullite matrix (Loryuenyong *et. al.*, 2013). It can be viewed as like sheets wrapping the mullite grains to connect a carbon network (CN) as shown in figure 7d. Also, the graphite phase can be found in any interstices of ceramic grains in the composite compact. Finally, the densification of the ceramic particles as an effect of sintering was evident for samples sintered at 1250$^{o}$C (figure 7d-encircled) which corroborate with the increased bulk density.

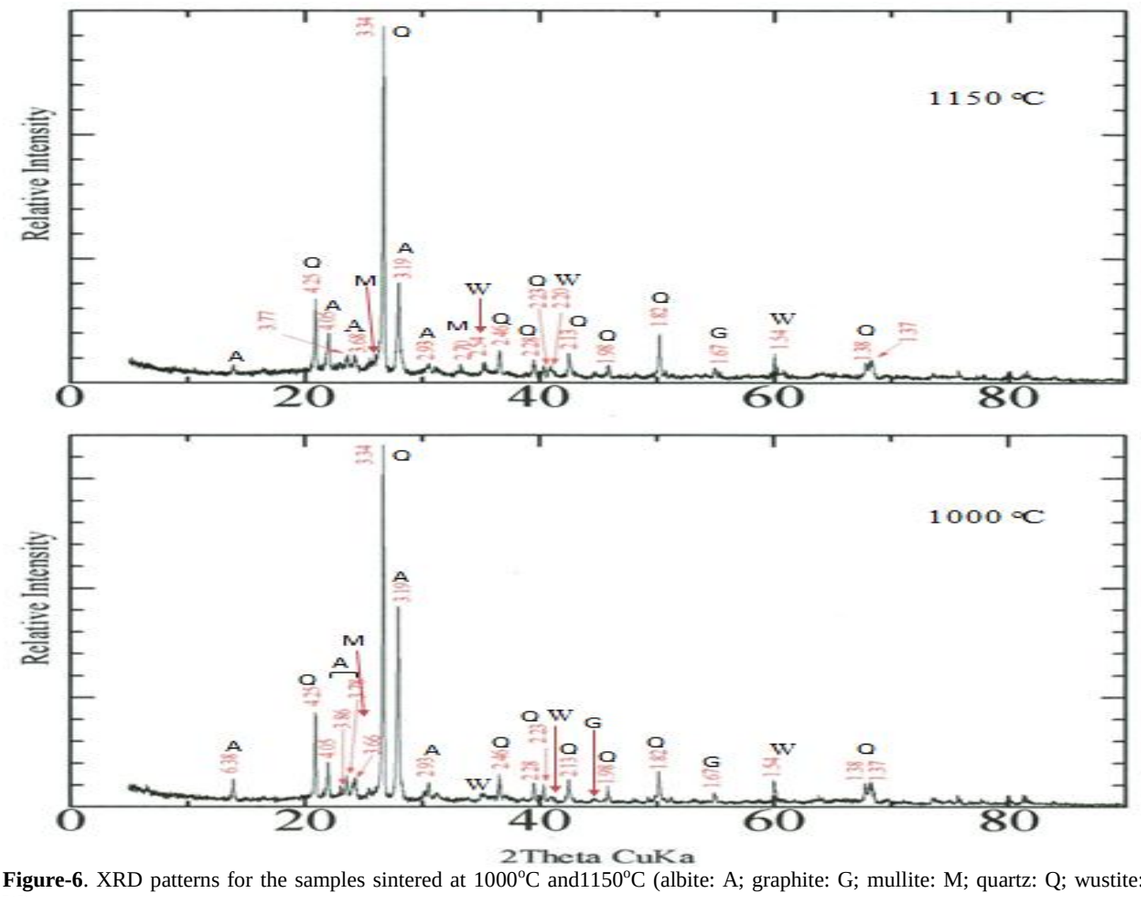


**Figure-6**. XRD patterns for the samples sintered at 1000$^{o}$C and1150$^{o}$C (albite: A; graphite: G; mullite: M; quartz: Q; wustite: W).

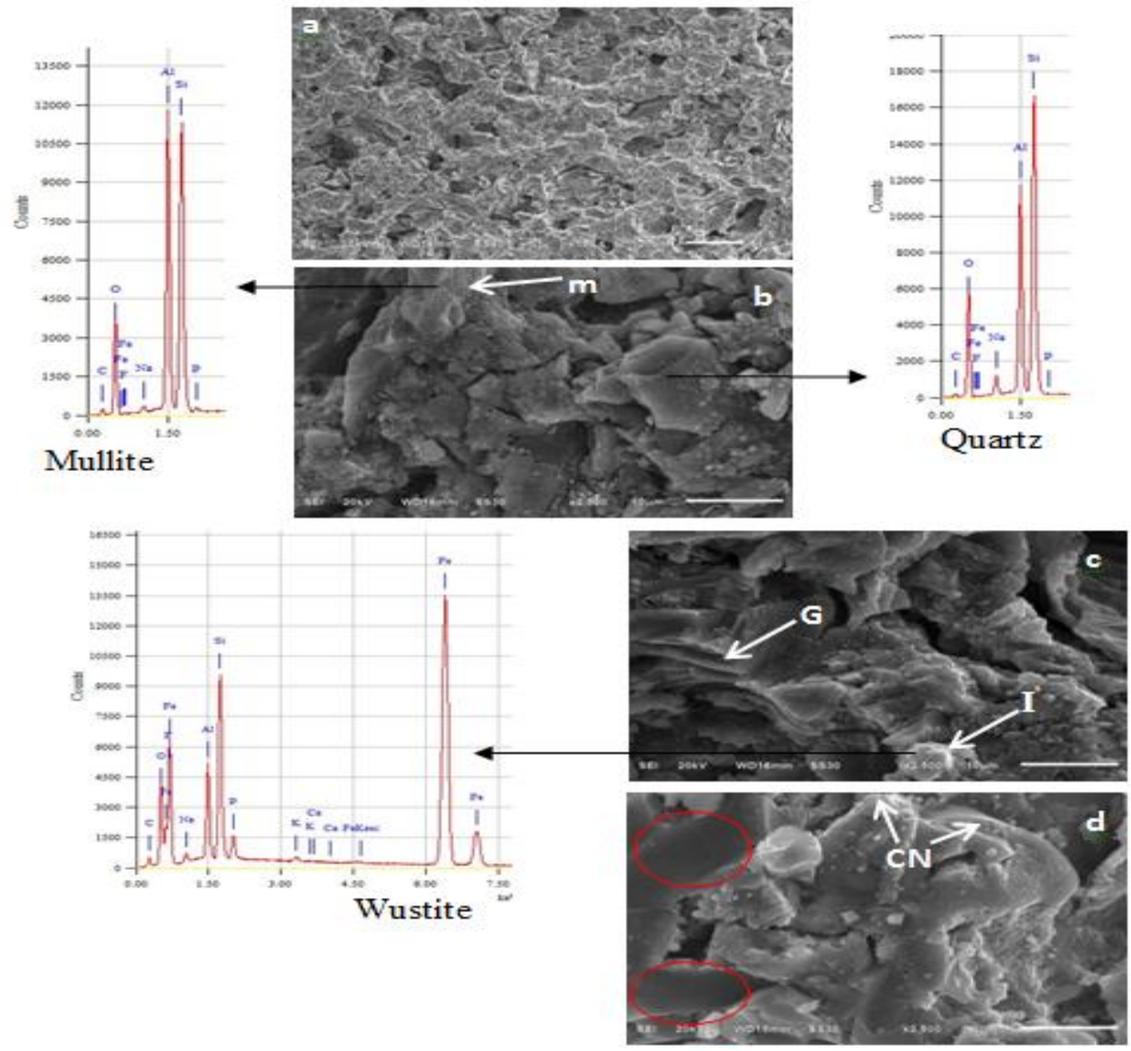


**Figure-7**. SEM images and EDS spectra of the ceramic composites sintered at: a) 1000$^{o}$C; b) 1150 $^{o}$C, mullite m, quartz: Q; c) 1200$^{o}$C, graphite: G, wustite:W; and d) 1250$^{o}$C.

## 4. Conclusion

A clay-based ceramic/carbon composite was successfully synthesized by starch consolidation casting and reductive sintering. This method presents a simple, less expensive and eco-friendly synthesis of the ceramic/carbon composite. The pyrolyzed carbon was in the form of graphite phase with a decreasing carbon yield (3.96-1.27%) as the sintering temperature increases. The electrical measurements continue to increase from 1.16-3.91 S/cm despite the reduction in carbon content. The XRD analysis revealed the presence of wustite that might reinforce the conduction networks of graphite and affected the electrical property of the samples. The mullite phase was also formed in the sintered composite along with other phases including quartz, albite feldspar at the lower sintering temperature. The reduction of porosity might also contribute to the enhancement of electrical conductivity. The physical properties of the fired samples revealed decreasing apparent porosity with increasing bulk density as the firing temperature was increased. This trend corroborated with the increasing biaxial tensile strength. Subsequently, the physical properties of the newly synthesized ceramic/carbon composite suggest the potential of this material for use as a carbon-filled ceramic water filter or as electrode materials.

## 5. Acknowledgement

The authors are thankful to MSU-Iligan Institute of Technology (MSU-IIT), Philippines and DOST-Engineering Research and Development for Technology (ERDT) for the support and funding of this research.

## References

Al-Lami, H. & Al-Rawi, W. (2008). Effect of forming methods on the properties of controlled porous ceramics, Eng.&Tech., 26(1).

Chen, C., Lan, G., & Tuan, W. (2000). Microstructural evolution of mullite during the sintering of kaolin powder compacts. Ceram. Int., 26, 715-720.

Choudhury, T. & Misra, N.M. (2011). Role of clay as catalyst in Friedel-Craft Alkylation. Bulletin of Materials Science, 34 (6), 1273-79.

Criado, M., Fernandez-Jimenez, A., & A. Palomo. (2007). Alkali activation of fly ash: Effect of the $SiO_2/Na_2O$ ratio Part I: FTIR study. Microporous and Mesoporous Materials, 106, 180–191.

Loryuenyong, V., Totepvimarn, K., Eimburanapravat, P., Boonchompoo, W., & Buasri, A. (2013). Preparation and characterization of educed graphene oxide sheets via water-based exfoliation and reduction methods. Advances in Materials Science and Engineering, Vol. 2013.

Lyckfeldt, 0. & Ferreirab, J. (1998). Processing of porous ceramics by starch consolidation. Journal of the European Ceramic Society, 18, 131-140.

Marquez, J., Rincon, J. & Romero, M. (2010). Mullite development on firing in porcelain stoneware bodies. Journal of the European Ceramic Society, 30(7), 1599-1607.

Menchavez, R. & Intong, L. (2010). Red clay-based porous ceramic with pores created by yeast-based foaming technique. J Mater Sci, 45, 6511-6520.

Menchavez, R., Fuji, M., & Takahashi, M. (2008) Electrically conductive dense and porous alumina with In-Situ-Synthesized nanoscale carbon networks. Advanced Materials, 20(12), 2345–2351.

Menchavez R.L., Fuji M., Shirai T., & Kumazawa T. (2014) Electrically conductive porous alumina/graphite composite synthesized by starch consolidation with reductive sintering. Journal of the European Ceramic Society, 34(3), 717-729.

Plaza, A., Buenavista, A., & Menchavez, R. (2014). Rapid starch consolidation of red clay-based ceramic slurry under simultaneous pressure-cooking and microwave irradiation. Ceramics International, 40(9): 14997.

Sun, C., & Guo, X. (2011). Electrical conductivity of MO(MO=FeO, NiO)-containing CaO-MgO-$SiO_2$-$Al_2O_3$ slag with low basicity. Transactions of Nonferrous Metals Society of China, 7(21), 1648-1654.

Treadwell, D., Dabbs, D., & Aksay, I. (1996). Mullite ($3Al_2O_3$-$2SiO_2$) synthesis with aluminosiloxanes. Chem. Mater., 8, 2056-2060.

Vyshnyakova1, K., Yushin, G., Pereselentseva, L., & Gogotsi, Y. (2006). Formation of porous SiC ceramics by pyrolysis of wood impregnated with Silica. Int. J. Appl. Ceram. Technol., 3(6), 485–490.

Zhao, S., Wang, C., Chen, M., & Sun, J. (2008). Mechanism for the preparation of carbon spheres from potato starch treated by $NH_4Cl$. Carbon, 47, 313–347.